University of Thi-Qar Journal of Science (UTsci)
ISSN Onlin:2709-0256, ISSN Print: 1991-8690 Volume (8), No.2,Oct.2021

# Effect of Direct Coupling on Electronic Transport and Thermoelectric Properties of Single Pyrene Molecule

Mohammed. N. Mutier
*Department of Physics/ Faculty of Science/ University of Thi Qar, Iraq*
Thi Qar, / Iraq
mo845692@gmail.com

Lafy F. Al-Badry
*Department of Physics/ Faculty of Science/ University of Thi Qar, Iraq*
Thi Qar, / Iraq
lafi.faraj_ph@sci.utq.edu.iq

***Abstract* — Electron transport characteristics through a single pyrene molecule, which connects with two metallic electrodes, are investigated by using of steady-state theoretical formalism. The transmission probability, I-V characteristics and thermoelectric properties are studied according to the influence of direct coupling between donor and acceptor. The new path between the donor and acceptor provides a direct route for the transfer of electrons between the donor and the acceptor, as well as the transfer of electrons across the molecule. We find the electronic transport properties improve by increasing donor-acceptor coupling factor.**

***Keywords— Electron transport; pyrene molecule; transmission probability; I-V characteristics; thermoelectric properties.***

## I. INTRODUCTION

Electron transport through single molecule has attracted much more attention since molecules constitute promising building blocks for future generation of electronic devices. Electron transport through single molecules was first studied theoretically in 1974 by Aviram and Ratner (Aviram & Ratner, 1974). It can be very significant in micro- and nanoscale charge transport. Indeed, phase coherence has been shown to be crucial to the observation of Aharanov-Bohm effects in microscopic metal rings (Webb *et al.* , 1985). The operation of such two-terminal devices gets due to applying a bias voltage. The transport properties of these systems are associated with some quantum effects, like as quantization of energy levels, quantum interference of electron waves (Baer & Neuhauser, 2002a, 2002b; Ernzerhof *et al*, 2006; Frauenheim *et al*., 2002; Goldsmith *et al.*, 2006; Launay & Coudret; Magoga & Joachim, 1999; Tagami *et al.*, 2003; Walter *et al*., 2004). The thermoelectric effects with improved efficiency can be thought as an alternative option for the future energy requirements (Ashcroft & Mermin, 1976; Ke *et al.*, 2009; Majumdar, 2004)**.** **T**he thermoelectric efficiency of a device is a dimensionless quantity as figure of merit, $ZT = S^2 G_e T/\kappa$, which is a function of thermopower (***S***), absolute temperature (**T**), electrical (**G**), and thermal (**κ**) conductances. The thermal conductance consists of two parts $\boldsymbol{\kappa} = \boldsymbol{\kappa}_{el} + \boldsymbol{\kappa}_{ph}$, where $\boldsymbol{\kappa}_{el}$ is the electronic thermal conductance and $\boldsymbol{\kappa}_{ph}$ indicate the phonon thermal conductance. In recent years, by progress of nanotechnology, it was found that in nanostructures, such as thin films and quantum dots, the thermoelectric properties significantly enhance (Harman *et al.*, 2002; Hsu et al., 2004; Venkatasubramanian *et al.*, 2001). Adding a thermal gradient or a coupling to a thermal bath (Entin-Wohlman ***et al.***, 2010; Jordan *et al.*, 2013), would also allow the molecules can be act as nano-scale thermoelectric devices (Dubi & Di Ventra, 2011). For instance, from the sign of *S* it is prospective to deduce if the Fermi level lies close to the highest occupied molecular orbital (HOMO) or the lowest unoccupied molecular orbital (LUMO)(Paulsson & Datta, 2003; Tan *et al.*, 2010). A positive (negative) sign denotes *p*-type (*n*-type) conduction, which means the Fermi level lies close the HOMO (LUMO). This implies that the sign and quantity of the thermopower can be changed through gating the molecule (Wang *et al.*, 2005; Wierzbicki & Świrkowicz, 2010; Zheng *et al.*, 2004). In this work, we calculate the electronic transport and thermoelectric properties of single pyrene molecule in case direct coupling between donor and acceptor. This configuration investigated for magnetic quantum ring and benzene molecule in Refs. (Patra & Maiti, 2017a, 2017b). Our calculations based on steady-state theoretical formalism to calculate transmission probability, electric current and thermoelectric properties of single pyrene molecule connected to two metallic electrodes. The outline of this article is as follows: The theoretical model is presented in Sec. 2, including the Hamiltonian which describes the on-site energies and coupling interactions among subsystems. In Sec. 3, we discuss our results, which include transmission probability, electric current and thermoelectric properties. The conclusion is concluded in Sec.4.

## II. THEORETICAL MODEL

The considered system is presented in Fig.1, the pyrene molecule is asymmetrically connected between donor and acceptor as ortho configuration, where the donor (acceptor) connected to first (second) atomic site. Which encouraged us to examine the electron transport in the case of direct

coupling between the donor and acceptor. The Hamiltonian which describes this system can be written as,

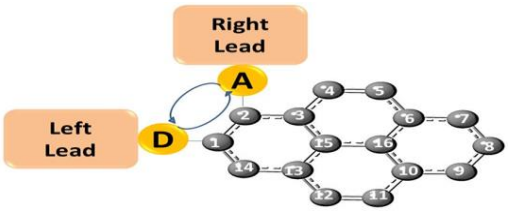


Fig. 1. An illustration of pyrene molecule attached to donor and acceptor at first and second atomic sites, respectively. The donor connected to left lead and the acceptor connected to right lead. the arrow refers to direct coupling between donor and acceptor.

$$H(t) = H_E(t) + H_{DMA}(t) + H_{LR}(t), \quad (1)$$

where,

$$H_E(t) = \sum_{\alpha=D,A} E_\alpha n_\alpha(t) + \sum_{m=1}^{16} E_m n_m(t) + \sum_{\beta=L,R} E_{k_\beta} n_{k_\beta}(t) \dots (2a)$$

describes energy levels of all subsystems, where $E_\alpha$ are donor (α=D) and acceptor ($\alpha = A$) levels, $E_m$ is on-site energies of pyrene molecule $m = (1, \dots, 16)$, $E_{k_\beta}$ are energy levels of left lead ($\beta = L$), and right lead ($\beta = R$). The energy level of atomic site (11) can be controlled by gate voltage as $E_{11} = E_0 + V_g$, where $E_0$ is eginvalue of atomic site (11). The coupling interactions between subsystems are given by Hamiltonian,

$$H_{DMA}(t) = V_{D1} C_D^\dagger(t) C_1(t) + V_{A,2} C_A^\dagger(t) C_2(t) + V_{D,A} C_D^\dagger(t) C_A(t) + \sum_{i,j} V_{ij}\, C_i^\dagger(t) C_j(t) + H.C \quad (2b)$$

$V_{D1}$ represents the coupling interaction between the donor and the first atomic site, the coupling interaction between the acceptor and second atomic site is $V_{A,2}$, and $V_{ij}$ is the nearest-neighbor hopping integral between the atomic sites in pyrene molecule.

$$H_{LR}(t) = \sum_{k_L} V_{Dk_L}\, C_D^\dagger(t) C_{k_L}(t) + \sum_{k_R} V_{A,k_R}\, C_A^\dagger(t) C_{k_R}(t) + H.C \quad (2c)$$

$V_{Dk_L}(V_{Ak_R})$ represent the tunneling between donor (acceptor) and left lead (right lead). The index $k_\beta$ describes a set of quantum numbers of the left and right leads. The occupation number is $n_j(t) = C_j^\dagger(t) C_j(t)$ and the $C_j^\dagger(t)$ and $C_j(t)$ denote creation and annihilation operators. By using the following formula (Abbas ***et al.***, 2017; Ballentine, 2014),

$$\dot{C}_j(t) = -i \frac{dH(t)}{dC_j^\dagger(t)} \quad (3)$$

The equations of motion can be written as:

$$\dot{C}_D(t) = -iE_D C_D(t) - iV_{D1} C_1(t) - iV_{D,A} C_A(t) - i \sum_{k_L} V_{Dk_L} C_{k_L}(t) \quad (4)$$

$$\dot{C}_A(t) = -iE_A C_A(t) - iV_{A,2} C_2(t) - iV_{A,D} C_D(t) - i \sum_{k_R} V_{Ak_R} C_{k_R}(t) \quad (5)$$

$$\dot{C}_{k_L}(t) = -i \sum_{k_L} E_{k_L} C_{k_L}(t) - iV_{k_L D} C_D(t) \quad (6)$$

$$\dot{C}_{k_R}(t) = -i \sum_{k_R} E_{k_R} C_{k_R}(t) - iV_{k_R A} C_A(t) \quad (7)$$

$$\dot{C}_1(t) = -iE_1 C_1(t) - iV_{1,D} C_D(t) - iV_{1,2} C_2(t) - iV_{1,14} C_{14}(t) \quad (8)$$

$$\dot{C}_2(t) = -iE_2 C_8(t) - iV_{2,A} C_A(t) - iV_{2,1} C_1(t) - iV_{2,3} C_3(t) \quad (9)$$

$$\dot{C}_{16}(t) = -iE_{16} C_{16}(t) - iV_{16,6} C_6(t) - iV_{16,10} C_{10}(t) - iV_{16,15} C_{15}(t) \quad (10)$$

$$\dot{C}_3(t) = -iE_3 C_3(t) - iV_{3,2} C_2(t) - iV_{3,4} C_4(t) - iV_{3,15} C_{15}(t) \quad (11)$$

$$\dot{C}_6(t) = -iE_6 C_6(t) - iV_{6,5} C_5(t) - iV_{6,7} C_7(t) - iV_{6,16} C_{16}(t) \quad (12)$$

$$\dot{C}_{10}(t) = -iE_{10} C_{10}(t) - iV_{10,9} C_9(t) - iV_{10,11} C_{11}(t) - iV_{10,16} C_{16}(t) \quad (13)$$

$$\dot{C}_{13}(t) = -iE_{13} C_{13}(t) - iV_{13,12} C_{12}(t) - iV_{13,14} C_{14}(t) - iV_{13,15} C_{15}(t) \quad (14)$$

$$\dot{C}_{15}(t) = -iE_{15} C_{15}(t) - iV_{15,3} C_3(t) - iV_{15,13} C_{13}(t) - iV_{15,16} C_{16}(t) \quad (15)$$

$$\dot{C}_n(t) = -iE_n C_n(t) - iV_{n,n+1} C_{n+1}(t) - iV_{n,n-1} C_{n-1}(t) \quad (16)$$

The system approaches a steady state at long time, where $C_j(t)$ are time dependent coefficients which can become time independent coefficients by using formula (Lafy F Al-Badry, 2017; Mohammed A. Abbas, 2017):

$$C_j(t) = \bar{C}_j(E) e^{-iEt} \quad (17)$$

With $E$ denotes the eigenvalues of system. By deriving Eq. (17) as a function of time, that Eqs. (4)- (16) can be rearranged as a matrix,

$$\begin{vmatrix} X_1 & V & 0 & 0 & 0 & 0 & 0 & 0 & 0 & 0 & 0 & 0 & 0 & V & 0 & 0 \\ V & X_2 & V & 0 & 0 & 0 & 0 & 0 & 0 & 0 & 0 & 0 & 0 & 0 & 0 & 0 \\ 0 & V & X_3 & V & 0 & 0 & 0 & 0 & 0 & 0 & 0 & 0 & 0 & 0 & V & 0 \\ 0 & 0 & V & X_4 & V & 0 & 0 & 0 & 0 & 0 & 0 & 0 & 0 & 0 & 0 & 0 \\ 0 & 0 & 0 & V & X_5 & V & 0 & 0 & 0 & 0 & 0 & 0 & 0 & 0 & 0 & 0 \\ 0 & 0 & 0 & 0 & V & X_6 & V & 0 & 0 & 0 & 0 & 0 & 0 & 0 & 0 & V \\ 0 & 0 & 0 & 0 & 0 & V & X_7 & V & 0 & 0 & 0 & 0 & 0 & 0 & 0 & 0 \\ 0 & 0 & 0 & 0 & 0 & 0 & V & X_8 & V & 0 & 0 & 0 & 0 & 0 & 0 & 0 \\ 0 & 0 & 0 & 0 & 0 & 0 & 0 & V & X_9 & V & 0 & 0 & 0 & 0 & 0 & 0 \\ 0 & 0 & 0 & 0 & 0 & 0 & 0 & 0 & V & X_{10} & V & 0 & 0 & 0 & 0 & V \\ 0 & 0 & 0 & 0 & 0 & 0 & 0 & 0 & 0 & V & X_{11} & V & 0 & 0 & 0 & 0 \\ 0 & 0 & 0 & 0 & 0 & 0 & 0 & 0 & 0 & 0 & V & X_{12} & V & 0 & 0 & 0 \\ 0 & 0 & 0 & 0 & 0 & 0 & 0 & 0 & 0 & 0 & 0 & V & X_{13} & V & V & 0 \\ V & 0 & 0 & 0 & 0 & 0 & 0 & 0 & 0 & 0 & 0 & 0 & V & X_{14} & 0 & 0 \\ 0 & 0 & V & 0 & 0 & 0 & 0 & 0 & 0 & 0 & 0 & 0 & V & 0 & X_{15} & V \\ 0 & 0 & 0 & 0 & 0 & V & 0 & 0 & 0 & V & 0 & 0 & 0 & 0 & V & X_{16} \end{vmatrix} \times \begin{vmatrix} \bar{C}_1 \\ \bar{C}_2 \\ \bar{C}_3 \\ \bar{C}_4 \\ \bar{C}_5 \\ \bar{C}_6 \\ \bar{C}_7 \\ \bar{C}_8 \\ \bar{C}_9 \\ \bar{C}_{10} \\ \bar{C}_{11} \\ \bar{C}_{12} \\ \bar{C}_{13} \\ \bar{C}_{14} \\ \bar{C}_{15} \\ \bar{C}_{16} \end{vmatrix} = \begin{vmatrix} V_{1,D}\bar{C}_D \\ V_{2,A}\bar{C}_A \\ 0 \\ 0 \\ 0 \\ 0 \\ 0 \\ 0 \\ 0 \\ 0 \\ 0 \\ 0 \\ 0 \\ 0 \\ 0 \\ 0 \end{vmatrix} \quad (18)$$

Where $X_m = E - E_m$, from Eq. (18), the coefficients $\bar{C}_J(E)$ are found by,

$$\bar{C}_2(E) = \frac{[\Delta_{2,A}\bar{C}_A + \Delta_{2,D}\bar{C}_D]}{\Delta} \quad (19)$$

Where $\Delta$ represents the first determinant of the left side, while, $\Delta_{2,A}$ and $\Delta_{2,D}$ are two determinants and can be obtained by substituting right side from Eq. (18) in the column2 of determinant $\Delta$.

By using Eqs. (5), (7), (17) and (19) we get transmission probability amplitude,

$$t(E) = \frac{\bar{C}_A(E)}{\bar{C}_D(E)} = \frac{V_{A,2}\ \Delta_{2,D} + \Delta V_{A,D}}{\Delta(E - E_A) - (V_{A,2}\ \Delta_{2,A}) - \Delta \sum_{AR}(E)} \quad (20)$$

Where $\sum_{AR}(E) = \Delta_R(E) - i\frac{1}{2}\Gamma_R(E)$ is the self-energy function which describes the effect of the leads and the coupling interactions on the electron dynamics(Al-Badry, 2016). The width function $\Gamma_R(E)$ is the imaginary part of the self-energy function, $\Delta_R(E)$ is level-shift function. The transmission probability $T(E)$ can be given by the following relation:

$$T(E) = |t(E)|^2 \quad (21)$$

In the following, to calculate the thermoelectric properties of our system, firstly the charge and heat currents can written as follows, respectively:

$$I = \frac{2e}{h}\int \big(f_L(E) - f_R(E)\big)T(E)dE \quad (22)$$

$$Q = \frac{2}{h}\int (E - \mu_L)(f_L(E) - f_R(E))T(E)dE \quad (23)$$

The charge and heat currents, in linear response regime, can be given by:

$$I = e^2K_0\Delta V + \frac{e}{T}K_1\Delta T \quad (24)$$

$$Q = eK_1\Delta V + \frac{1}{T}K_2\Delta T \quad (25)$$

where e is the charge of electron, $T$ the absolute temperature, and transport coefficients are computed from the integral:

$$K_n(\mu, T) = \frac{1}{h}\int(-\frac{\partial f}{\partial E})(E - \mu)^n T(E)dE \quad (26)$$

with $h$ is Planck constant, $\mu$ is the chemical potential and $f_\beta(E) = 1/1 + exp\left(\frac{E-\mu_\beta}{k_B T_\beta}\right)$ is the Fermi distribution function for the lead $\beta$ $(= L, R)$ and $k_B$ being the Boltzmann constant.

So, the electric conductance $G$, thermopower$S$, electron thermal conductance $\kappa_{el}$and figure of merit $ZT$ are given by:

$$G = e^2K_0 \quad (27)$$

$$S = -\frac{1}{eT}\frac{K_1}{K_0} \quad (28)$$

$$\kappa_{el} = \frac{1}{T}\left(K_2 - \frac{K_1^2}{K_0}\right) \quad (29)$$

$$ZT = \frac{S^2GT}{\kappa_{el} + \kappa_{ph}} \quad (30)$$

While the phonon thermal conductance, $\kappa_{ph}$, is neglected in our study as it compares to with $\kappa_{el}$. Thus, the figure of merit is written as:

$$ZT = \frac{1}{\frac{K_0K_2}{K_1^2} - 1} \quad (31)$$

## III. Results and Discussion

The eV units are used of measuring energies and coupling strengths in considered system. The on-site energies of the carbon atoms in the pyrene molecule were $E_m = 0$, the energy levels of donor and acceptor were $E_D = E_A = 0$, the width of the conduction band of left and right leads is define by $4\beta$ where $\beta = -3\ eV$. The nearest-neighbor hopping strengths among atomic sites are $V = -2.4\ eV$ (Abbas et al., 2017), and coupling interactions between donor with left lead and acceptor with right lead $V_{k_LD} = V_{k_RA} = v = -3\ eV$, coupling interactions between donor with the first atomic site and acceptor with the second atomic site are $V_{D1} = V_{A2} = -1\ eV$.

### *A. Transmission probability*

The transmission spectrum for pyrene molecule has been calculated in case direct coupling between donor and acceptor with several values of donor-acceptor coupling interaction, as indicated in Fig. 2. The number of resonances in the transmission spectrum under the effect of direct coupling is constant. In addition, the direct coupling effect decreases antiresonance in the transmission spectrum. Furthermore, the transmission probability gradually increases by increasing $\tau$ at $E = E_F$ has the following order :$T(\tau = 1.5) > T(\tau = 1) > T(\tau = 0.5) > T(\tau = 0)$. At all values of $\tau$, fine resonant peaks associated with energy eigenvalues of the pyrene molecule are obtained while the transmission probability drops very close to zero for all other energies. We observe that the transmission spectrum behaves entirely opposite behavior before and after resonant

peaks. One side of resonant peaks, the transmission probability gradually increases while in the other side it suddenly decreases by increasing the donor-acceptor coupling. It is significant feature since one can get higher and/or lower transmission at different energies simply by controlling the donor-acceptor coupling, without varying any other physical variables. The anomalous feature in pyrene molecule-like geometry is observed due to the presence of the new path between the donor and acceptor. This behavior observed in Ref. (Patra & Maiti, 2017b)

The two antiresonances for all values of donor-acceptor coupling appear at $E = \pm 1eV$ . While donor-acceptor coupling leads to shift the antiresonances located at other energies. The antiresonances reduced due to increasing the donor-acceptor coupling. A combined interference effect among electronic waves passing through different arms (upper and lower arms of the molecular ring) including the external new path. Thus, a competition takes place between the interfering paths i.e., the molecular arms and the external path. Therefore, both paths are responsible for transmission probability and collective effect obtained at the right lead. The electrons follow the external path when the coupling interaction between the electrodes is enoughly strong, avoiding the path across the molecule.

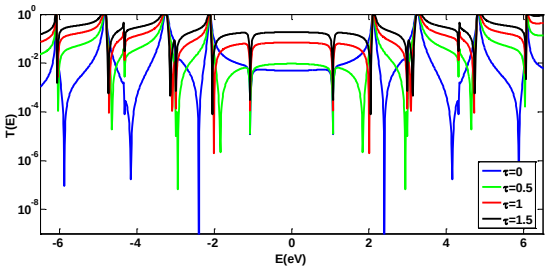


Fig. 2. Transmission probability as a function of electron energy injunction in pyrene molecule in case direct coupling with several values of donor-acceptor coupling $\tau = 0, 0.5, 1, 1.5eV$ .

## B. *Electric current*

In order to provide a deep understanding of the electron transport, we have calculate the electric current as a function of bias voltage in the range from $-8V$ to $8V$ with several values of donor-acceptor coupling, as indicated in Fig. 3. In case non equilibrium, that a bias voltage is applied to the leads, which positioned the quantized energy levels of pyrene molecule within bias window. Therefore, current will flow between the two leads through the molecule. With the increase of the bias voltage, the chemical potentials of the metallic leads are moved gradually and lastly cross one of the quantized energy levels of the pyrene molecule. As a result, the electric current behaves as staircase at resonant peaks of the transmission spectrum.

The influence of direct coupling is not noticeable at $\boldsymbol{\tau = 0.5}$, the electric current of both values of $\boldsymbol{\tau = 0}$ ,and $\boldsymbol{0.5}$ are perfectly corresponding, because the electron needs a strong reaction for the purpose of crossing through the external path between the donor and the acceptor, in this case ($\boldsymbol{\tau = 0.5}$), the electron mainly will follow the internal path through the molecule. The amplitude of electric current increases and access to 12 at $\boldsymbol{\tau = 1}$, which confirms that the electron began to follow the external path between the donor and the acceptor, in addition to the internal path. An interesting feature of the electric current appears at $\boldsymbol{\tau = 1.5}$, the electric current linearly increases in conductance gap at a range of gate voltage $\boldsymbol{-4 < V < 4}$, as well as, the amplitude increases sharply with $\boldsymbol{\tau}$ and accesses to 20. This behavior observed in Ref. (Patra & Maiti, 2017b)

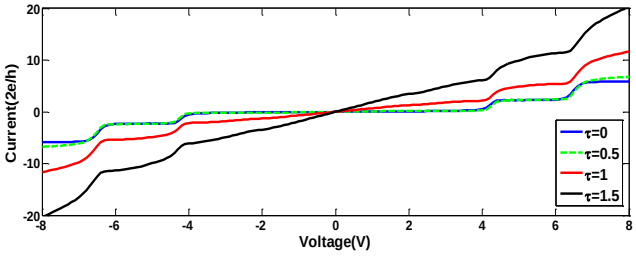


Fig. 3. The electric current as a function of bias voltage in pyrene molecule with several values of donor-acceptor coupling $\tau = 0, 0.5, 1, 1.5$ .

## C. *Thermoelectric properties*

In this section, we concentrate on the variations of the thermoelectric properties as a function gate voltage applied to pyrene molecule, as presented in Fig. 4. In the linear response regime, the temperature $T_L = T_R = T = 300K$ and chemical potential $\mu_L = \mu_R = 0$ of the left and right leads.

We see the electrical conductance increases with the increasing values of $\tau$, as shown in Fig. 4(a). The electrical conductance of values $\tau = 0, 0.5$ vanishes in the range from -2 to 2V, while it of value $\tau = 1.5$ not vanishes in the entire range of gate voltage. From Fig. 4(b), the thermopower will decrease with the increasing values of $\tau$. Therefore, the behavior of electron thermal conductance similar to that of electrical conductance as a function of the gate voltage applied to pyrene molecule, where will increase by increasing values of $\tau$, as presented in Fig. 4(c). As noticeable, the thermal conductance not vanishes in all values of gate voltage at $\tau = 1,1.5$. However, the figure of merit vanishes about Fermi level for all values of $\tau$, as shown in Fig. 4(d). While it accesses to 0.21 in case absence the coupling interaction between the donor and acceptor at $Vg = \pm 1V$, as presented in the inset of Fig. 4(d), as well as, it access to 7 at $Vg = \pm 6V$.

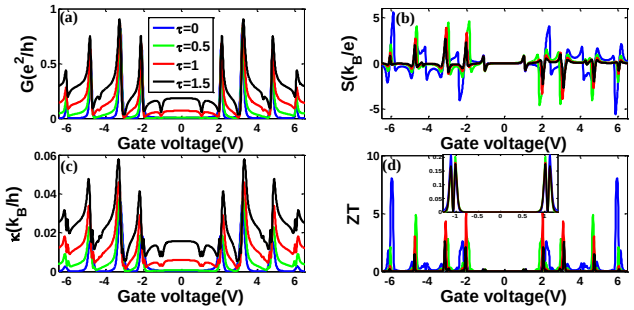


Fig. 4. Thermoelectric properties **as a function of gate voltage** of pyrene molecule **(a) electrical conductance**, *(b)* **thermopower** , *(c)* thermal conductance and (d) figure of merit with several values of donor-acceptor coupling $\tau = 0, 0.5, 1, 1.5$ .

In summary, the electron transport and thermoelectric properties of the pyrene molecule, has been calculated in case direct coupling between donor and acceptor with several values of donor-acceptor coupling interaction. The direct coupling leads to reducing antiresonance in the transmission spectrum. Furthermore, the transmission probability gradually increases by increasing τ at Fermi energy. In addition, In case of direct coupling, an interesting feature of the electric current appears at τ=1.5, the electric current linearly increases in conductance gap at a range of gate voltage -4<V< 4, as well as, the amplitude access to 20. Which confirms that the electron began to follow the external path between the donor and the acceptor. Finally, the electrical conductance and thermal conductance under direct coupling increase with the increasing values of τ. While the thermopower will reduce with the increasing values of τ .However, the figure of merit vanishes about Fermi level for all values of τ, while it access to 0.21 in case τ=0 at $Vg = \pm 1V$.

## REFERENCES


**Abbas, M. A., Hanoon, F. H., & Al-Badry, L. F. (2017).** Theoretical study of electron transport throughout some molecular structures. On *Superlattices and Microstructures*, *111*, *273-285*.

**Al-Badry, L. F. (2016).** The influence of the nanostructure geometry on the thermoelectric properties. *Physica E: Low-dimensional Systems and Nanostructures*, *83*, 201-206.

**Al-Badry, L. F. (2017).** The electronic properties of concentric double quantum ring and possibility designing XOR gate. *Solid State Communications*, *254*, 15-20.

**Ashcroft, N., & Mermin, N. (1976).** Solid State Physics, Holt, Rinehart and Winston. *New York*.

**Aviram, A., & Ratner, M. A. (1974).** Molecular rectifiers. *Chemical Physics Letters*, *29*(2), 277-283.

**Baer, R., & Neuhauser, D. (2002a).** Anti-coherence based molecular electronics: XOR-gate response. *Chemical Physics*, *281*(2-3), 353-362.

**Baer, R., & Neuhauser, D. (2002b).** Phase coherent electronics: a molecular switch based on quantum interference. *Journal of the American Chemical Society*, *124*(16), 4200-4201.

**Ballentine, L. E. (2014).** *Quantum Mechanics: A Modern Development Second Edition*: World Scientific Publishing Company.

**Dubi, Y., & Di Ventra, M. (2011).** Colloquium: Heat flow and thermoelectricity in atomic and molecular junctions. *Reviews of Modern Physics*, *83*(1), 131.

**Entin-Wohlman, O., Imry, Y., & Aharony, A. (2010).** Three-terminal thermoelectric transport through a molecular junction. *Physical Review B*, *82*(11), 115314.

**Ernzerhof, M., Bahmann, H., Goyer, F., Zhuang, M., & Rocheleau, P. (2006).** Electron transmission through aromatic molecules. *Journal of chemical theory and computation*, *2*(5), 1291-1297.

**Frauenheim, T., Seifert, G., Elstner, M., Niehaus, T., Köhler, C., Amkreutz, M., . . . Suhai, S. (2002).** Atomistic simulations of complex materials: ground-state and excited-state properties. *Journal of Physics: Condensed Matter*, *14*(11), 3015.

**Goldsmith, R. H., Wasielewski, M. R., & Ratner, M. A. (2006).** Electron Transfer in Multiply Bridged Donor− Acceptor Molecules: Dephasing and Quantum Coherence. *The Journal of Physical Chemistry B*, *110*(41), 20258-20262.

**Harman, T., Taylor, P., Walsh, M., & LaForge, B. (2002).** Quantum dot superlattice thermoelectric materials and devices. *science*, *297*(5590), 2229-2232.

**Hsu, K. F., Loo, S., Guo, F., Chen, W., Dyck, J. S., Uher, C., . . . Kanatzidis, M. G. (2004).** Cubic AgPbmSbTe2+ m: bulk thermoelectric materials with high figure of merit. *science*, *303*(5659), 818-821.

**Jordan, A. N., Sothmann, B., Sánchez, R., & Büttiker, M. (2013).** Powerful and efficient energy harvester with resonant-tunneling quantum dots. *Physical Review B*, *87*(7), 075312.

**Ke, S.-H., Yang, W., Curtarolo, S., & Baranger, H. U. (2009).** Thermopower of molecular junctions: An ab initio study. *Nano letters*, *9*(3), 1011-1014.

**Launay, J., & Coudret; A. Aviram and MA Ratner** C. Molecular Electronics, eds. *(Academy of Sciences, New York, 1998)*.

**Magoga, M., & Joachim, C. (1999).** Conductance of molecular wires connected or bonded in parallel. *Physical Review B*, *59*(24), 16011.

**Majumdar, A. (2004).** Thermoelectricity in semiconductor nanostructures. *science*, *303*(5659), 777-778.

**Mohammed A. Abbas, F. H. H., Lafy F. Al-Badry. (2017).** Possibility designing XNOR and NAND molecular logic gates by using single benzene ring. *Solid State Communications*, *263* 42–49.

**Patra, M., & Maiti, S. K. (2017a).** Externally controlled high degree of spin polarization and spin inversion in a conducting junction: Two new approaches. *Scientific Reports*, *7*(1), 14313.

**Patra, M., & Maiti, S. K. (2017b).** Modulation of circular current and associated magnetic field in a molecular junction: A new approach. *Scientific reports*, *7*, 43343.

**Paulsson, M., & Datta, S. (2003).** Thermoelectric effect in molecular electronics. *Physical Review B, 67*(24), 241403.

**Tagami, K., Tsukada, M., Matsumoto, T., & Kawai, T. (2003).** Electronic transport properties of free-base tape-porphyrin molecular wires studied by self-consistent tight-binding calculations. *Physical Review B, 67*(24), 245324.

**Tan, A., Sadat, S., & Reddy, P. (2010).** Measurement of thermopower and current-voltage characteristics of molecular junctions to identify orbital alignment. *Applied Physics Letters, 96*(1), 013110.

**Venkatasubramanian, R., Siivola, E., Colpitts, T., & O'quinn, B. (2001).** Thin-film thermoelectric devices with high room-temperature figures of merit. *Nature, 413*(6856), 597.

**Walter, D., Neuhauser, D., & Baer, R. (2004).** Quantum interference in polycyclic hydrocarbon molecular wires. *Chemical Physics, 299*(1), 139-145.

**Wang, B., Xing, Y., Wan, L., Wei, Y., & Wang, J. (2005).** Oscillatory thermopower of carbon chains: First-principles calculations. *Physical Review B, 71*(23), 233406.

**Webb, R. A., Washburn, S., Umbach, C., & Laibowitz, R. (1985).** Observation of h e aharonov-bohm oscillations in normal-metal rings. *Physical Review Letters, 54*(25), 2696.

**Wierzbicki, M., & Świrkowicz, R. (2010).** Enhancement of thermoelectric efficiency in a two-level molecule. *Journal of Physics: Condensed Matter, 22*(18), 185302.

**Zheng, X., Zheng, W., Wei, Y., Zeng, Z., & Wang, J. (2004).** Thermoelectric transport properties in atomic scale conductors. *The Journal of chemical physics, 121*(17), 8537-8541.